

# Miniature fiber-tip photoacoustic spectrometer for trace gas detection

Yingchun Cao, Wei Jin,\* Hoi Lut Ho, and Jun Ma

Department of Electrical Engineering, The Hong Kong Polytechnic University, Hong Kong, China

\*Corresponding author: [eewjin@polyu.edu.hk](mailto:eewjin@polyu.edu.hk)

Received November 27, 2012; revised December 13, 2012; accepted January 4, 2013;

posted January 4, 2013 (Doc. ID 180709); published February 8, 2013

We demonstrate a fiber-tip photoacoustic spectrometric sensor for trace gas detection. The sensor head is a miniature fiber-tip hollow-cavity with a deflectable polymer diaphragm. Periodic light absorption of gas molecules within the cavity generates an acoustic pressure wave, which causes deflection of the diaphragm. The hollow cavity also is a Fabry–Perot interferometer with which the diaphragm deflection is detected with high sensitivity. Experimental test around the P(9) absorption line of  $C_2H_2$  achieved a minimum detectable gas concentration of 4.3 ppm with an excitation laser power of 8 mW. The miniature sensor head and fiber optic detection system make this type of spectrometers ideally suited for remote and space-limited applications as well as for multipoint detection in a multiplexed fiber optic sensor network. © 2013 Optical Society of America

OCIS codes: 060.2370, 280.4788, 300.6260.

Photoacoustic (PA) spectroscopy (PAS), in which periodic light absorption of gas molecules is converted into acoustic pressure wave via the PA effect, has been studied extensively for high-sensitivity trace gas detection [1,2]. However, in most PAS systems reported so far, the generated acoustic waves were detected by electrical means such as capacitive microphones [3,4] and resonant quartz tuning forks [5–7]. Microcantilever in combination with a free-space optical Michelson interferometer also was investigated for PA detection and has achieved very high detection sensitivity [8,9]. However, free-space optics are unsuitable for long-distance transmission, and electrical cables were used for transmission to/from the sensor head (the PA cell). Although gas concentration detection up to parts-per-billion (ppb) level has been achieved [3,7,9], the electric nature of the detection methods renders them less than ideal for environments with electromagnetic interference and for large-scale sensor networks.

Using a fiber optic-based microphone for PA detection has been investigated. Breguet *et al.* used a long length of coiled optical fiber together with a Sagnac interferometer to detect the acoustic signal [10]. Wang *et al.* developed a diaphragm-based Fabry–Perot interferometric (FPI) acoustic sensor and integrated it into a PA cell for gas detection [11]. With a polymer diaphragm of  $\sim 4$  mm in diameter, a 500 mW excitation laser power, they demonstrated the detection of  $C_2H_2$  gas with a minimum detectable concentration of 1.56 ppb.

In this Letter, we report what we believe is a novel fiber-tip, diaphragm-based FPI system for PAS gas detection. In this system, PA wave generation occurs inside the hollow cavity of the FPI, while acoustic detection is achieved with the same FPI through the pressure-induced deflection of the diaphragm. The system was successfully used for  $C_2H_2$  gas detection and achieved a favorable lower concentration detection limit, while the size of the sensor head is reduced down to  $\sim$ mm scale, which is significantly smaller than previously reported PAS systems.

Figure 1 is a schematic of the sensor head. It is an extrinsic FPI (EFPI) with a polymer diaphragm.

A microchannel is introduced from the side of the cavity to allow gas to diffuse in and out. Light from a wavelength-modulated laser source (excitation laser) is delivered to the hollow cavity via a single mode fiber (SMF) and acoustic pressure wave is generated within the cavity through the PA effect. The FPI is formed between the end of the SMF and the surface of the polymer diaphragm. The reflected light signals from these two surfaces interferes with each other and the acoustically induced diaphragm deflection changes the EFPI cavity length, which can be interrogated by a second laser (the probe laser).

To sensitively detect the acoustic wave, it is important to have sensitive diaphragms [12,13]. We used a thin polymer with low Young's modulus (0.138 GPa) as the diaphragm material. The fabrication process of the sensor head is illustrated in Fig. 2 [14]. A drop of polyimide (Norland, NOA 68) with volume of  $\sim 4$  mm<sup>3</sup> is dispensed into deionized water in a Petri dish and spreads out into a thin layer of liquid film floating on the water surface [Fig. 2(a)]. The size of the polymer layer is determined from its coloration by controlling the spreading time. The polymer is then UV-cured when its diameter reaches  $\sim 5$  cm. Thus, a solid polymer film with a thickness of  $\sim 2$   $\mu$ m is obtained. The film is then lifted out with a support and heated in an oven (set to 50°C) to evaporate the residual water in it. Then a plastic structure is carefully fabricated to act as the outer ferrule. The main section of the ferrule has an inner diameter of 2.5 mm, while the frontier section has a slightly larger diameter

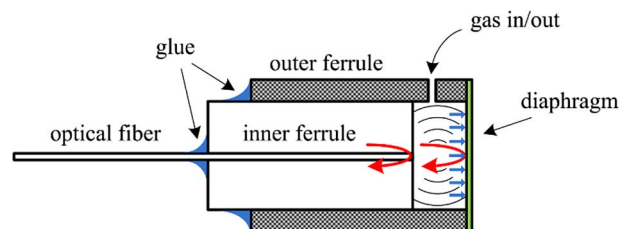


Fig. 1. (Color online) Schematic of the miniature fiber-tip sensor head. An EFPI is formed between the fiber end of the diaphragm.

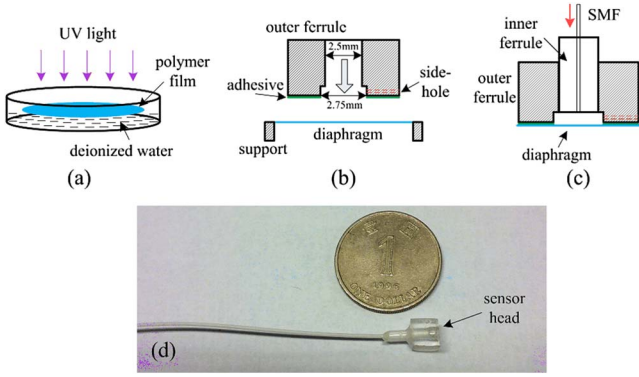


Fig. 2. (Color online) (a)–(c) Schematics showing the fabrication process of the sensor head. (d) Photo of the sensor head.

(2.75 mm) to leave some space for the gas diffusion. A 1.48 mm diameter side hole is made at the frontier section of the ferrule to facilitate gas diffusion into the cavity. The ferrule end is first covered with a thin layer of adhesive and then moved toward the polymer diaphragm [Fig. 2(b)] until the diaphragm is stuck to the ferrule end. Then an inner ferrule with inner/outer diameter of 125  $\mu\text{m}$ /2.5 mm is used to hold the SMF and form hollow cavity. The SMF, with its end cleaved, is inserted into the inner ferrule until its end is on the same plane of the inner ferrule endface and then it is fixed with glue. The inner ferrule together with the SMF is then inserted into the outer ferrule step by step with the help of a translation stage [Fig. 2(c)]. The reflection from the low-finesse FPI, formed between the SMF end and the polymer diaphragm, is monitored by using a broadband light source in combination with an optical spectrum analyzer until the desired cavity length is achieved. Finally, a photo of the sensor head is shown in Fig. 2(d). The reflection spectrum of the polymer-diaphragm-based EFPI prepared for the following gas-sensing experiment is shown in Fig. 3. The visibility of the interference fringe is over 12 dB with a free spectrum range of  $\sim 6.9$  nm around 1550 nm, which corresponds to a Fabry–Perot cavity length of 172  $\mu\text{m}$  [15].

Figure 4 shows the experimental setup for the fiber-tip PAS system. A distributed feedback (DFB) laser with wavelength of 1.53  $\mu\text{m}$  and output power of 8 mW is used as the excitation laser ( $\lambda_e$ ) for PA generation. The wavelength of the DFB laser is sinusoidally modulated by an

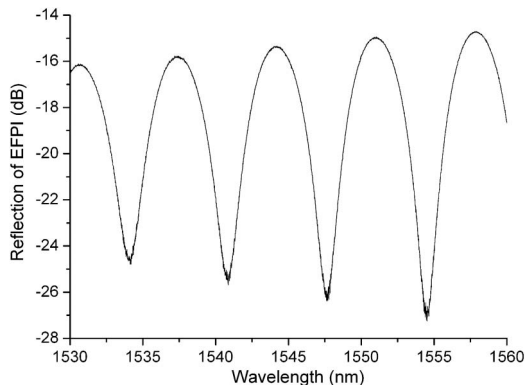


Fig. 3. Reflection spectrum of the diaphragm-based EFPI prepared for PAS gas sensing.

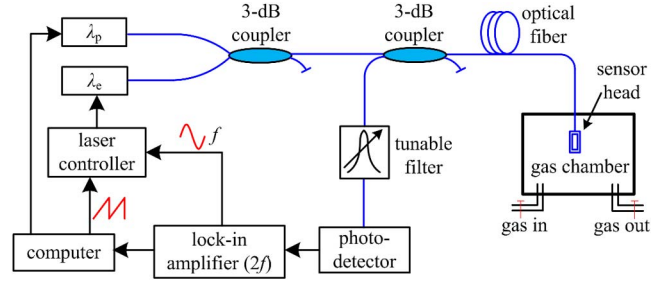


Fig. 4. (Color online) Experimental setup of the fiber-tip PAS gas detection system. The blue lines show the optical path while the black lines show the electrical path. The detailed structure of the sensor head is given in Fig. 1.  $\lambda_e$  and  $\lambda_p$  denote the excitation laser and probe laser, respectively.

internal signal generator of a lock-in amplifier and simultaneously swept across the P(9) absorption line of  $\text{C}_2\text{H}_2$  via computer control.

Rather than resonating in a one-dimensional open tube like many of the previous PAS systems [3–7], we use a miniature, closed-cavity PA cell and make it work in a regime of nonacoustic resonance. The pressure-induced periodic diaphragm deflection is monitored by a probe laser ( $\lambda_p$ ) with output power of  $\sim 4$  mW. The wavelength of the probe laser is tuned to 1556.1 nm, corresponding to a linear response region with the largest slope in the Fabry–Perot interference fringe. A tunable bandpass wavelength filter is used to block the reflected light at the excitation wavelength, while the reflected probe light, after passing through the bandpass filter, is received by a photodetector and demodulated by a lock-in amplifier at its second harmonic. The time constant of the lock-in amplifier was set to 10 s, associated with a 24 dB/octave filter slope. The wavelength of the probe laser should be properly selected to avoid crossover with the excitation laser.

Wavelength modulation with  $2f$  detection is used in this method. The modulation frequency was set to 200 Hz, which generates an acoustic pressure wave at its second harmonic in the gas absorption line center. This frequency is found to fall within a flat frequency response region of the polymer diaphragm. All the experiments were carried out at atmospheric pressure and room temperature. With the excitation laser wavelength swept across the P(9) absorption line of  $\text{C}_2\text{H}_2$ , by laser temperature tuning, the second harmonic PA signal detected by the lock-in amplifier for 1%  $\text{C}_2\text{H}_2$  gas balanced by  $\text{N}_2$  is plotted in Fig. 5. It is shown that a peak-to-peak PA signal of 616.44  $\mu\text{V}$  is achieved for our setup. The noise level is deduced from the standard deviation in the nonabsorption region as 0.27  $\mu\text{V}$  ( $1\sigma$ ). Therefore, a signal-to-noise ratio of 2314 is estimated, which corresponds to a minimum detectable gas concentration of 4.3 ppm. The asymmetry of the signal profile is due to the effect of residual amplitude modulation [16].

Experiments also were carried out for various  $\text{C}_2\text{H}_2$  concentrations obtained by mixing a standard source gas (1%  $\text{C}_2\text{H}_2$ ) with pure  $\text{N}_2$  at different volume ratios controlled by two mass flow meters. The measured second harmonic PA signal for different gas concentration is plotted in Fig. 6 as black squares. Curve fitting shows that the PA signal has an excellent linear relationship

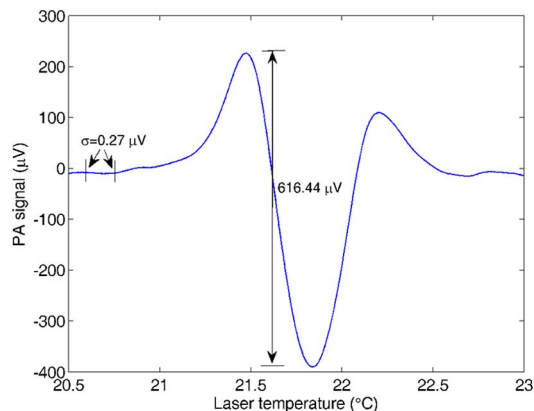


Fig. 5. (Color online) Second harmonic signal detected around the P(9) absorption line of  $C_2H_2$  gas. The gas concentration is 1%.

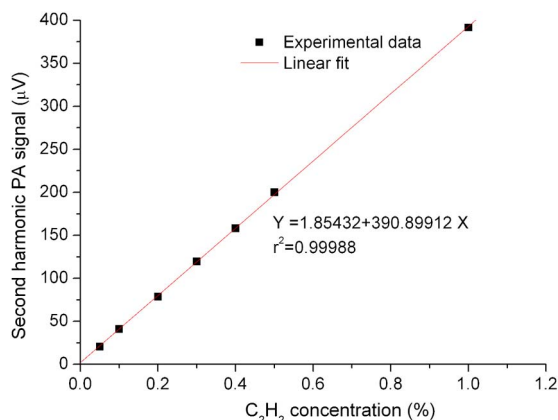


Fig. 6. (Color online) Dependence of second harmonic PA signal on gas concentration.

( $r^2 = 0.99988$ ) with the gas concentration in the range of 0.05%–1%.

In conclusion, we demonstrated what we believe is a novel fiber-tip PA spectrometer for trace gas detection with a diaphragm-based FPI. Since both generation and detection of the PA wave are localized in a miniature Fabry–Perot cavity, the size of the sensor head and the volume of sample can be greatly reduced compared to previous PAS systems. By using a thin polymer diaphragm as the acoustic detector and an 8 mW DFB laser

as the light source for PA excitation, we experimentally demonstrated the detection of  $C_2H_2$  gas with a minimum detectable concentration of 4.3 ppm. The detection performance could be further improved by optimizing the dimension and the material of the diaphragm using a higher excitation laser power. The miniaturized sensor head and the fiber optic format for excitation and detection of PA wave would make these spectrometers especially useful for remote and space-limited applications and for multipoint gas detection in a multiplexed fiber optic sensor network.

We acknowledge the support of the Hong Kong SAR Government through a GRF grant PolyU 5096/09E, and The Hong Kong Polytechnic University through grant J-BB9K.

## References

1. A. Miklós, P. Hess, and Z. Bozóki, *Rev. Sci. Instrum.* **72**, 1937 (2001).
2. C. Haisch, *Meas. Sci. Technol.* **23**, 012001 (2012).
3. M. E. Webber, M. Pushkarsky, and C. K. N. Patel, *Appl. Opt.* **42**, 2119 (2003).
4. A. A. I. Khalil, M. A. Gondal, and N. Al-Suliman, *Appl. Phys. B* **103**, 441 (2011).
5. A. A. Kosterev, Y. A. Bakhrin, R. F. Curl, and F. K. Tittel, *Opt. Lett.* **27**, 1902 (2002).
6. A. A. Kosterev, F. K. Tittel, D. V. Serebryakov, A. L. Malinovsky, and I. V. Morozov, *Rev. Sci. Instrum.* **76**, 043105 (2005).
7. L. Dong, A. A. Kosterev, D. Thomazy, and F. K. Tittel, *Appl. Phys. B* **100**, 627 (2010).
8. K. Wilcken and J. Kauppinen, *Appl. Spectrosc.* **57**, 1087 (2003).
9. V. Koskinen, J. Fonsen, K. Roth, and J. Kauppinen, *Vib. Spectrosc.* **48**, 16 (2008).
10. J. Breguet, J. P. Pellaux, and N. Gisin, *Sens. Actuators A Phys.* **48**, 29 (1995).
11. Q. Wang, J. Wang, L. Li, and Q. Yu, *Sens. Actuators B Chem.* **153**, 214 (2011).
12. E. Cibula and D. Donlagic, *Appl. Opt.* **44**, 2736 (2005).
13. J. Ma, W. Jin, H. L. Ho, and J. Y. Dai, *Opt. Lett.* **37**, 2493 (2012).
14. S. Nesson, M. Yu, and X. Zhang, *J. Biomed. Opt.* **13**, 044040 (2008).
15. J. Xu, X. Wang, K. L. Cooper, and A. Wang, *Opt. Lett.* **30**, 3269 (2005).
16. Y. Cao, W. Jin, H. L. Ho, L. Qi, and Y. Yang, *Appl. Phys. B* **109**, 359 (2012).